DØ note 4833-CONF

Simultaneous measurement of $\mathcal{B}(\mathbf{t \to Wb})/\mathcal{B}(\mathbf{t \to Wq})$ and $\sigma(\mathbf{p\bar{p} \to t\bar{t}})$ at DØ

The DØ Collaboration
URL http://www-d0.fnal.gov

(Dated: June 15, 2005)

We present the simultaneous measurement of the branching ratio $R = \mathcal{B}(t \to Wb)/\mathcal{B}(t \to Wq)$ together with the top quark pair ($t\bar{t}$) production cross section ($\sigma_{t\bar{t}}$) in $p\bar{p}$ collisions at $\sqrt{s} = 1.96$ TeV, using 230 pb^{-1} of data collected by the DØ experiment at the Fermilab Tevatron Collider. We select events with one charged lepton ℓ (electron or muon), missing transverse energy ($\not\!\!E_T$), and three or four jets in the final state. We employ lifetime-based b-jet identification techniques to count the number of ℓ+ jet + $\not\!\!E_T$ events with 0, 1 and 2 b-jets. A likelihood discriminant based on the kinematical properties of $t\bar{t}$ events is used to further constrain the number of $t\bar{t}$ events without lifetime-tagged jets. We measure $R = 1.03^{+0.19}_{-0.17}$ (stat + syst) and $\sigma_{t\bar{t}} = 7.9^{+1.7}_{-1.5}$ (stat + syst) $\pm$ 0.5(lumi) pb, in good agreement with the standard model expectation.

Preliminary Results for Summer 2005 Conferences

I. INTRODUCTION

The CKM matrix element $\mid V_{tb} \mid$ is indirectly constrained by the measurement of other CKM matrix elements, to the interval $0.9990 <\mid V_{tb} \mid< 0.9992$ at the 90% C.L. [1] based on the assumption of the unitarity of the CKM matrix. In this case the ratio of branching fractions $R= \mathcal{B}(t \to Wb)/\mathcal{B}(t \to Wq)$ can be expressed in terms of CKM matrix elements:

$$R = \frac{\mid V_{tb} \mid^2}{\mid V_{tb} \mid^2 + \mid V_{ts} \mid^2 + \mid V_{td} \mid^2} =\mid V_{tb} \mid^2 \tag{1}$$

In the framework of the Standard Model (SM), the ratio R is therefore constrained to be in the interval 0.9980-0.9984 at the 90% C.L. [1]. The non-unitarity of the CKM matrix could for example arise from the existence of a fourth quark generation and lead to a deviation of R from unity. The CDF collaboration had measured R in Run I [2], $R = 0.94^{+0.31}_{-0.24}$ (stat + syst), and recently in Run II [3], $R = 1.12^{+0.27}_{-0.23}$ (stat + syst), finding in both cases a result consistent with the SM prediction, yet statistics limited.

Experimentally, R can be determined by selecting a sample enriched in $t\bar{t}$ events, here with a high p_T isolated lepton, large missing transverse energy and three, four or more jets. The selected events are categorized into events with 0, 1 and 2 or more lifetime-tagged jets. From the number of observed events in the three categories and the kinematics of events with no lifetime-tagged jet, we fit R and the $t\bar{t}$ pair production cross section .

In this paper, we report the measurement of $\mathcal{B}(t \to Wb)/\mathcal{B}(t \to Wq)$ and $\sigma_{t\bar{t}}$ in the lepton (electron or muon) plus jets channel using b-jet identification (b-tagging) techniques exploiting the long lifetime of B hadrons. The data were collected by the DØ experiment from August 2002 through March 2004, and correspond to an integrated luminosity of 226 ± 15 pb^{-1} (229 ± 15 pb^{-1}) in the electron (muon) sample. The determination of the sample composition relies on the background calculations and the tagging efficiencies determined in the $t\bar{t}$ cross section measurement using lifetime tagging [4] on the same data set.

II. DØ DETECTOR

The DØ detector includes a tracking system, calorimeters, and a muon spectrometer [5]. The tracking system consists of a silicon microstrip tracker (SMT) and a central fiber tracker (CFT), both located inside a 2 T superconducting solenoid. The tracker design provides efficient charged particle measurements in the pseudorapidity region $|\eta| < 3$ [6]. The SMT strip pitch of 50–80 μm allows a precise reconstruction of the primary interaction vertex (PV) and an accurate determination of the impact parameter of a track relative to the PV [7], which are the key components of the lifetime-based b-jet tagging algorithms. The PV is required to be within the SMT fiducial volume and consist of at least 3 tracks. The calorimeter consists of a central section (CC) covering $|\eta| < 1.1$, and two end calorimeters (EC) extending the coverage to $|\eta| \approx 4.2$. The muon system surrounds the calorimeter and consists of three layers of tracking detectors and two layers of scintillators [9]. A 1.8 T iron toroidal magnet is located outside the innermost layer of the muon detector. The luminosity is calculated from the rate for $p\bar{p}$ inelastic collisions detected using two hodoscopes of scintillation counters mounted close to the beam pipe on the front surfaces of the EC calorimeters.

III. EVENT PRESELECTION

We select data samples in the electron and muon channels by requiring an isolated electron with $p_T > 20$ GeV and $|\eta| < 1.1$, or an isolated muon with $p_T > 20$ GeV and $|\eta| < 2.0$. More details on the lepton identification as well as trigger requirements are reported elsewhere [10]. In both channels, we require $\not\!\!E_T$ to exceed 20 GeV and not be collinear with the lepton direction in the transverse plane. These W boson candidate events must be accompanied by one or more jets with $p_T > 15$ GeV and rapidity $|y| < 2.5$ [6]. Jets are defined using a cone algorithm with radius $\Delta\mathcal{R} = 0.5$ [11]. We classify the selected events according to their jet multiplicity. Events with 3 or ≥ 4 jets are expected to be enriched in $t\bar{t}$ signal, whereas events with only 1 or 2 jets are expected to be dominated by background. We use the former to estimate $\mathcal{B}(t \to Wb)/\mathcal{B}(t \to Wq)$ and $\sigma_{t\bar{t}}$, and the latter to verify the background normalization procedure.

The main background in this analysis is the production of W bosons in association with jets (W+jets), with the W boson decaying leptonically. In most cases, the jets accompanying the W boson originate from light (u, d, s) quarks and gluons (W+light jets). Depending on the jet multiplicity, between 2% and 14% of W+jets events contain heavy flavor jets resulting from gluon splitting into $b\bar{b}$ or $c\bar{c}$ ($Wb\bar{b}$ or $Wc\bar{c}$, respectively), while in about 5% of events, a single c quark is present in the final state as a result of the W boson radiated from an s quark from the proton's or

antiproton's sea (Wc). A sizeable background arises from strong production of two or more jets ("multijets"), with one of the jets misidentified as a lepton and accompanied by large $\not\!\!E_T$ resulting from mismeasurements of jet energies. Significantly smaller contributions to the selected sample arise from single top, Z+jets, and weak diboson (WW, WZ and ZZ) production. Together these backgrounds are expected to contribute from 1% to 7% of the selected sample depending on the number of lifetime-tagged jets and are refered to as "other" backgrounds.

The normalization of the various backgrounds starts by the determination of the number of multijet events in the selected sample. The multijet background is determined using control samples from data and probabilities for jets to mimic isolated lepton signatures also determined from data [10]. This method allows to determine the fraction of events with a real isolated high p_T lepton ($t\bar{t}$ and all backgrounds except multijet background) and the fraction of events from the multijet background. The contribution from single top, Z+jet and weak diboson production are determined from Monte Carlo simulation. The remainder of the selected sample is either $t\bar{t}$ or W+jet production. Since tagging probabilities for $t\bar{t}$ events and W+jets are different, we can let fluctuate both the $t\bar{t}$ and the W+jets absolute contributions when we fit $\mathcal{B}(t \to Wb)/\mathcal{B}(t \to Wq)$ and $\sigma_{t\bar{t}}$ to the data.

IV. LIFETIME-TAGGING

A. Secondary vertex tagging

We use a secondary vertex tagging (SVT) algorithm to identify b-quark jets. Secondary vertices are reconstructed from two or more tracks satisfying the following requirements: $p_T > 1$ GeV, ≥ 1 hits in the SMT layers and impact parameter significance $d_{ca}/\sigma_{d_{ca}} > 3.5$ [7]. Tracks identified as arising from K^0_S or Λ decays or from γ conversions are not considered. If the secondary vertex reconstructed within a jet has a decay length significance $L_{xy}/\sigma_{L_{xy}} > 7$ [8], the jet is tagged as a b-quark jet. Events with exactly 1 (≥ 2) tagged jets are referred to as single-tag (double-tag) events. Events with exactly 0 tagged jet are referred to as zero-tag events. A description of how b-tagging, c-tagging and light-jet tagging efficiencies are computed can be found in [4] along with the procedure to calculate the event tagging probabilities for the background processes and for $t\bar{t}$ events with $\mathcal{B}(t \to Wb)/\mathcal{B}(t \to Wq) = 1$.

B. $t\bar{t}$ Event Tagging Probability for $\mathcal{B}(\mathbf{t \to Wb})/\mathcal{B}(\mathbf{t \to Wq}) \neq 1$

In the standard model case with $\mathcal{B}(t \to Wb)/\mathcal{B}(t \to Wq) = 1$ the $t\bar{t}$ event tagging probabilities are computed assuming that each of the signal events contains two b-jets. In the present analysis the $t\bar{t}$ event tagging probability becomes a function of $\mathcal{B}(t \to Wb)/\mathcal{B}(t \to Wq)$. In general, for $R \neq 1$, a $t\bar{t}$ event might have 0, 1 or 2 b-jets from the two top quark decays, strongly affecting the event tagging probability and how $t\bar{t}$ events are distributed among the zero-, single- and double-tag samples. To derive the $t\bar{t}$ event tagging probability as function of R we determine the event tagging probability in the three following scenarios

1. $t\bar{t} \to W^+b\ W^-\bar{b}$ (further will be referred to as $tt \to bb$)
2. $t\bar{t} \to W^+b\ W^-\bar{q}_\ell$ or its charge conjugate (referred to as $tt \to bq_\ell$)
3. $t\bar{t} \to W^+q_\ell\ W^-\bar{q}_\ell$ (referred to as $tt \to q_\ell q_\ell$),

where q_ℓ denotes either a d- or a s-quark. The probabilities $P_{\mathrm{n-tag}}$ to observe $\mathrm{n-tag} = 0$, 1 or ≥ 2 lifetime-tagged jets are computed separately for the three types of $t\bar{t}$ events, using the b-tagging efficiency for b-jets, c-tagging efficiency for c-jets and the light jet tagging probability for light flavor jets. The probabilities $P_{\mathrm{n-tag}}$ in the three scenarios are then combined in the following way to obtain the $t\bar{t}$ tagging probability as function of R

$$P_{\mathrm{n-tag}}(tt) = R^2 P_{\mathrm{n-tag}}(tt \to bb) + 2R(1-R)P_{\mathrm{n-tag}}(tt \to bq_\ell) + (1-R)^2 P_{\mathrm{n-tag}}(tt \to q_\ell q_\ell), \quad (2)$$

where the subscript n − tag runs over 0, 1 and ≥ 2 tags.

V. TOPOLOGICAL DISCRIMINANT IN THE ZERO-TAG SAMPLE

The fraction of $t\bar{t}$ events in the ℓ+ 4 jets zero-tag sample is between 10% for R=1 and 25% for R=0. This is not significanltly larger than the statistical error on the total number of events in the zero-tag sample. For this reason the information on the total number of observed events with zero-tag is a very poor constraint on

$\mathcal{B}(t \to Wb)/\mathcal{B}(t \to Wq)$ and $\sigma_{t\bar{t}}$. Without a stronger constraint on the number of $t\bar{t}$ events in the 0-tag sample a low value of $\mathcal{B}(t \to Wb)/\mathcal{B}(t \to Wq)$ and a rather large $t\bar{t}$ cross section (compared to a cross section measurement assuming $\mathcal{B}(t \to Wb)/\mathcal{B}(t \to Wq)$=1 [4]) are still allowed by the data. To fully exploit the zero-tag sample further discrimination is needed. To this end we construct a discriminant function that makes use of the differences between the kinematic properties of the $t\bar{t}$ events and the backgrounds. We selected a set of four variables, well modelled by simulation in samples depleted in top events and that provide good separation between signal and background. To reduce the dependence on modeling of soft radiation and underlying event, only the four highest p_T jets were used to determine these variables. The discriminant function is built from the following variables: *i*) the event sphericity $\mathcal{S}$, constructed from the four-momenta of the jets; *ii*) the event centrality $\mathcal{C}$, defined as the ratio of the scalar sum of the p_T of the jets to the scalar sum of the energy of the jets; *iii*) $K_{T\min} = \Delta R_{jj}^{\min} p_T^{\min}/E_T^W$, where $\Delta R_{jj}^{\min}$ is the minimum separation in $\eta - \phi$ space between pairs of jets, $p_T^{\min}$ is the p_T of the lower-p_T jet of that pair, and E_T^W is a scalar sum of the lepton transverse momentum and $\not\!\!E_T$; *iv*) $H_{T2}^{'}$, defined as the ratio H_{T2}/H_z, where H_{T2} is the scalar sum of the E_T for all jets excluding the leading jet and H_z is the scalar sum of the $|E_z|$ of all the jets plus the absolute value of the energy of the lepton and the neutrino along the z-direction. Sphericity and centrality characterize the event shape and are defined, for example, in Ref. [12].

The discriminant function was built using the method described in Ref. [13], and has the following general form:

$$\mathcal{D} \;=\; \frac{S(x_1, x_2, ...)}{S(x_1, x_2, ...) + B(x_1, x_2, ...)}\,, \tag{3}$$

where $x_1, x_2, ...$ is a set of input variables and $S(x_1, x_2, ...)$ and $B(x_1, x_2, ...)$ are the probability density functions for the $t\bar{t}$ signal and background, respectively. Neglecting the correlations between the input variables, the discriminant function can be approximated by the expression:

$$\mathcal{D} \;=\; \frac{\prod_i s_i(x_i)/b_i(x_i)}{\prod_i s_i(x_i)/b_i(x_i) + 1}\,, \tag{4}$$

where $s_i(x_i)$ and $b_i(x_i)$ are the normalized distributions of variable i for signal and background, respectively. As constructed, the discriminant function peaks near zero for the background, and near unity for the signal. The shape of the discriminant $\mathcal{D}$ is derived on simulated events for $t\bar{t}$ and W+jets events. For the multijet background the discriminant shape is obtained on a control sample of data events selected by requiring that the leptons fail the tightest lepton isolation criteria. The other backgrounds have kinematical properties close to the W+jet events and contribute to only 1% of the zero-tag sample. They are assumed to have the same discriminant shape as the W+jets events.

VI. RESULTS

To measure $\mathcal{B}(t \to Wb)/\mathcal{B}(t \to Wq)$ and $\sigma_{t\bar{t}}$ we perform a binned maximum likelihood fit to the data. The data is binned in: *i*) ten bins of the discriminant $\mathcal{D}$ in e + 4 jets zero-tag events, *ii*) ten bins of the discriminant $\mathcal{D}$ in μ + 4 jets zero-tag events, *iii*) two bins for the two zero-tag samples e+ 3 jets, μ+3 jets, *iv*) four bins for the four single-tag samples (electron or muon and 3 or 4 jets), *v*) four bins for the four double-tag samples (electron or muon and 3 or 4 jets). In each bin we make a prediction on the number of events which is the sum of the expected background and the signal contribution. The signal contribution is a function of R and $\sigma_{t\bar{t}}$. To predict the number of events in each bin of the discriminant $\mathcal{D}$ we use its expected shape for the backgrounds and the $t\bar{t}$ signal. The normalization of the multijet background is estimated by counting events in orthogonal samples [14]. The number of events in each control sample can fluctuate statistically. Therefore we use for each control sample an additional bin in the likelihood fit, to take into account statistical fluctuations in the multijet background calculation. The result is a likelihood function which is the product of 30 Poisson terms in the signal bins *i*) to *v*) and 12 Poisson terms in the twelve control bins (zero-tag, single-tag and double-tag, with 3 or 4 jets and for e + jet and μ + jet). We incorporate systematic uncertainties into the likelihood by using nuisance parameters [15]. All preselection efficiencies, tagging probabilities and shapes of the discriminant $\mathcal{D}$ become functions of the nuisance parameters. The final likelihood function contains one Gaussian term for each nuisance parameter. The values of $\mathcal{B}(t \to Wb)/\mathcal{B}(t \to Wq)$ and $\sigma_{t\bar{t}}$ that maximizes the total likelihood function are:

$$\begin{aligned} \mathcal{B}(t \to Wb)/\mathcal{B}(t \to Wq) \;&=\; 1.03^{+0.19}_{-0.17}\ (\text{stat} + \text{syst}) \\ \sigma_{t\bar{t}} \;&=\; 7.9^{+1.7}_{-1.5}\ (\text{stat} + \text{syst}) \pm 0.5(\text{lumi})\text{pb} \end{aligned} \tag{5}$$

Source	Uncertainty on $\mathcal{B}(t \to Wb)/\mathcal{B}(t \to Wq)$
Statistical	$+0.17\ -0.15$
Jet energy resolution	$+0.02\ -0.01$
Jet reconstruction and identification	± 0.03
b-tagging efficiency in Monte Carlo	± 0.02
b-tagging efficiency in data	$+0.06\ -0.05$
Flavor composition of W+jets background	$+0.03\ -0.02$
Kinematical properties of W+jets background	± 0.04
Others	$+0.04\ -0.02$
Total error	$+0.19\ -0.17$

TABLE 1: *Statistical and systematic uncertainties on $\mathcal{B}(t \to Wb)/\mathcal{B}(t \to Wq)$ in units of $\mathcal{B}(t \to Wb)/\mathcal{B}(t \to Wq)$.*

Source	Uncertainty on $\sigma_{t\bar{t}}$ (pb)
Statistical	$+1.4\ -1.3$
Lepton identification and trigger	$+0.4\ -0.3$
Jet energy scale	± 0.3
Jet energy resolution	± 0.1
Jet reconstruction and identification	± 0.2
b-tagging efficiency in data	± 0.1
Flavor composition of W+jets background	± 0.5
Kinematical properties of W+jets background	$+0.4\ -0.3$
Statistics in control samples	± 0.2
Others	$+0.2\ -0.1$
Total error	$+1.7\ -1.5$

TABLE 2: *Statistical and systematic uncertainties on $\sigma_{t\bar{t}}$ in pb.*

in good agreement with the standard model expectation. The statistical and dominant systematic uncertainties and their contributions are given in Table 1 and 2. The result of the 2-dimensional fit is shown in the plane ($\mathcal{B}(t \to Wb)/\mathcal{B}(t \to Wq)$, $\sigma_{t\bar{t}}$) in Figure 1, along with the 68% and 95% confidence level contours. In Fig. 2 we compare the observed number of events to the prediction obtained with $\mathcal{B}(t \to Wb)/\mathcal{B}(t \to Wq)$=1 and $\sigma_{t\bar{t}}$=7 pb in the zero-, single- and double-tag samples and for events with exactly three jets. Figure 3 shows the prediction and observation in events with 4 or more jets and in the zero-, single and double-tag sample. In Fig. 3 the zero-tag sample is split into the ten bins of the topological discriminant $\mathcal{D}$.

We also extract lower limits on R and the CKM matrix element $|V_{tb}|$ assuming $|V_{tb}| = \sqrt{R}$. Using a Bayesian approach with the following prior:

$$\pi(R) = \begin{cases} 1 & \text{if } 0 \le R \le 1 \\ 0 & \text{if } R < 0 \text{ or } R > 1 \end{cases}$$

we obtain $R > 0.81$ at 68% C.L. and $R > 0.64$ at 95% C.L. For the CKM matrix element $|V_{tb}|$ we obtain $|V_{tb}| > 0.90$ at 68% C.L. and $|V_{tb}| > 0.80$ at 95% C.L.

Acknowledgments

We thank the staff at Fermilab and collaborating institutions, and acknowledge support from the Department of Energy and National Science Foundation (USA), Commissariat à L'Energie Atomique and CNRS/Institut National de Physique Nucléaire et de Physique des Particules (France), Ministry for Science and Technology and Ministry for Atomic Energy (Russia), CAPES, CNPq and FAPERJ (Brazil), Departments of Atomic Energy and Science and Education (India), Colciencias (Colombia), CONACyT (Mexico), Ministry of Education and KOSEF (Korea), CONICET and UBACyT (Argentina), The Foundation for Fundamental Research on Matter (The Netherlands), PPARC (United Kingdom), Ministry of Education (Czech Republic), Natural Sciences and Engineering Research Council and WestGrid Project (Canada), BMBF (Germany), A.P. Sloan Foundation, Civilian Research and Development Foundation, Research Corporation, Texas Advanced Research Program, and the Alexander von Humboldt Foundation.

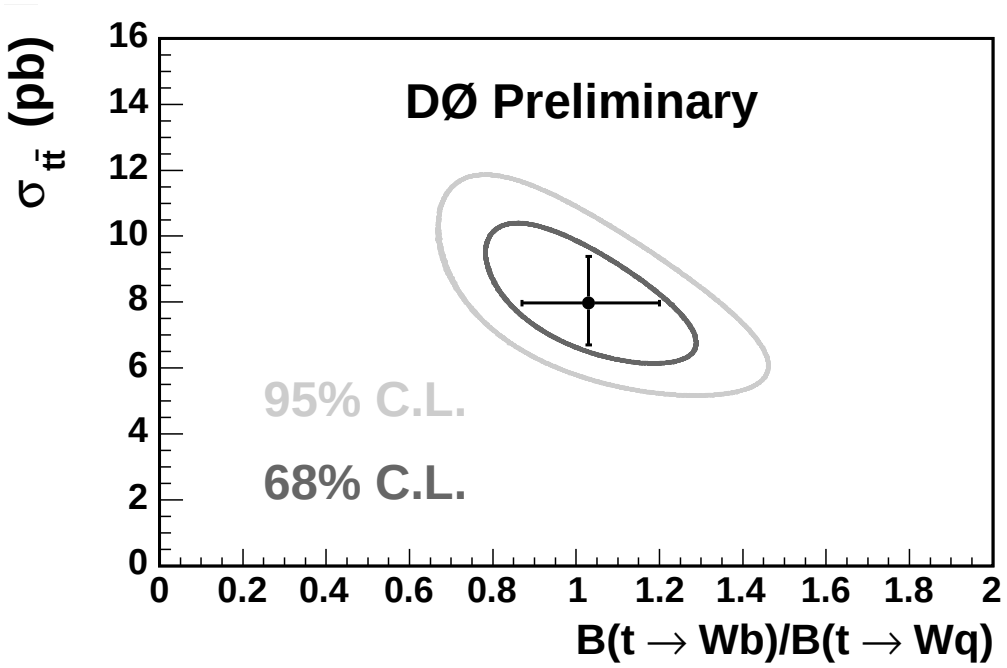

FIG. 1: *The 68% and 95% C.L. contours in the plane* ($\mathcal{B}(t \to Wb)/\mathcal{B}(t \to Wq)$, $\sigma_{t\bar{t}}$). *The point indicates the best fit to data*

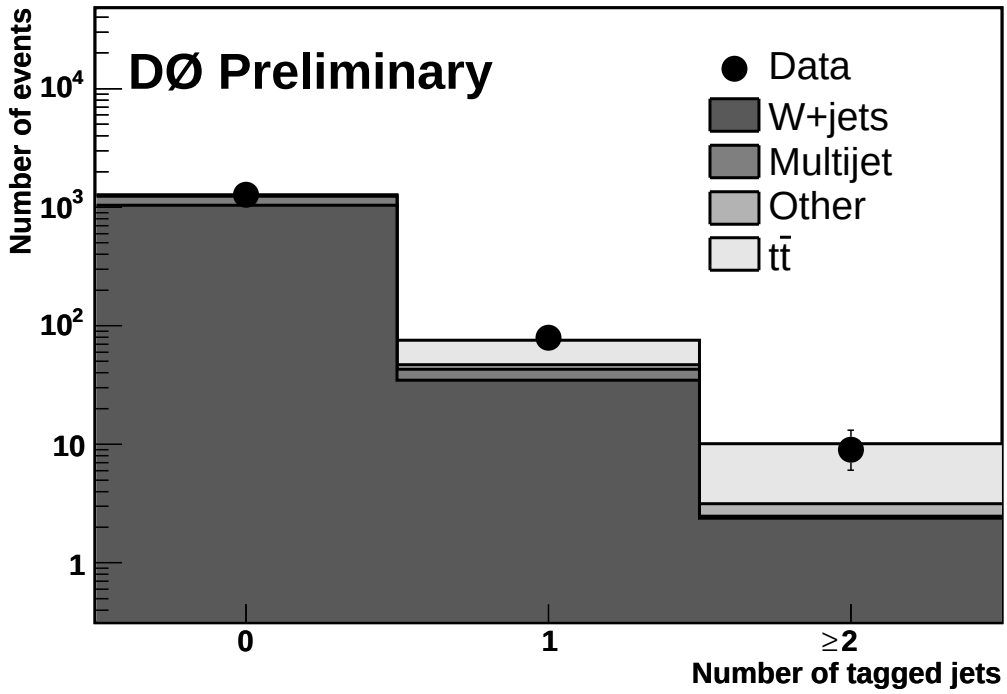

FIG. 2: *Predicted and observed number of events in* ℓ*+3 jets events in the zero-, single- and double-tag samples for* $\mathcal{B}(t \to Wb)/\mathcal{B}(t \to Wq)$*=1 and* $\sigma_{t\bar{t}}$*=7 pb.*

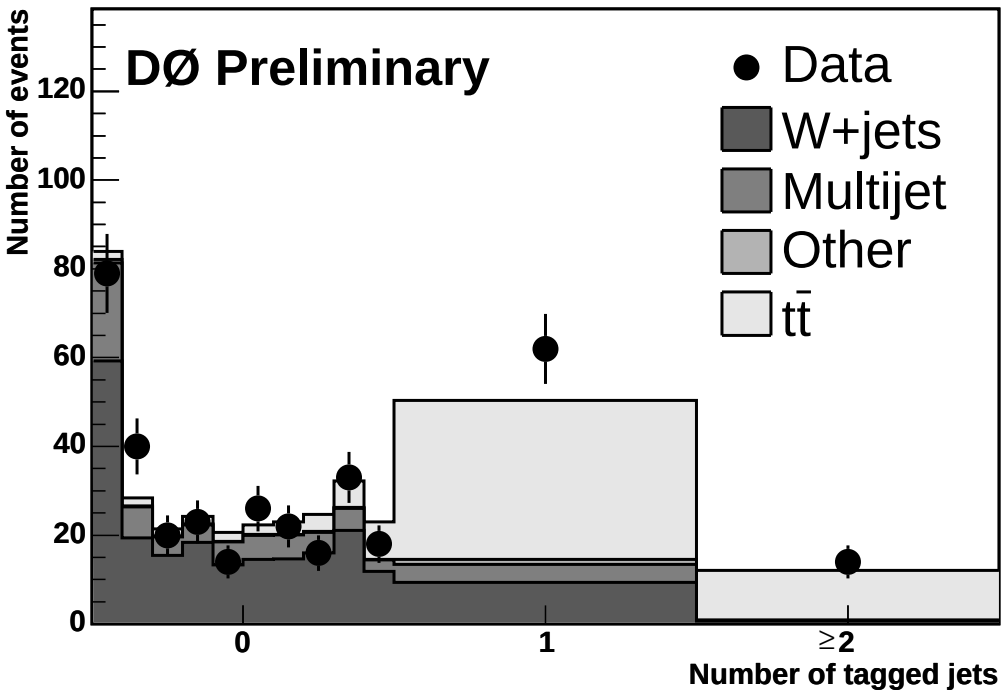

FIG. 3: *Predicted and observed number of events in ℓ+ 4 jets events, in the zero-, single- and double-tag samples for $\mathcal{B}(t \to Wb)/\mathcal{B}(t \to Wq)$=1 and $\sigma_{t\bar{t}}$=7 pb. The prediction and observation in the zero-tag sample are broken down into 10 bins of the topological discriminant $\mathcal{D}$.*

[1] S. Eidelman et al., Phys. Lett., B **592**, 1 (2004).
[2] CDF Collaboration, T. Affolder *et al.*, Phys. Rev. Lett. **86**, 3233 (2001).
[3] CDF Collaboration, T. Affolder *et al.*, submitted to Phys. Rev. Lett., hep-ex/0505091.
[4] DØ Collaboration, V. Abazov *et al.*, submitted to Phys. Lett. B, hep-ex/0504058.
[5] DØ Collaboration, V. Abazov *et al.*, "The Upgraded DØ Detector", in preparation for submission to Nucl. Instrum. Methods Phys. Res. A.
[6] Rapidity y and pseudorapidity η are defined as functions of the polar angle θ and parameter β as $y(\theta,\beta) \equiv \frac{1}{2}\ln\left[(1+\beta\cos\theta)/(1-\beta\cos\theta)\right]$ and $\eta(\theta) \equiv y(\theta,1)$, where β is the ratio of a particle's momentum to its energy.
[7] Impact parameter is defined as the distance of closest approach (d_{ca}) of the track to the primary vertex in the plane transverse to the beamline. Impact parameter significance is defined as $d_{ca}/\sigma_{d_{ca}}$, where $\sigma_{d_{ca}}$ is the uncertainty on d_{ca}.
[8] Decay length L_{xy} is defined as the distance from the primary to the secondary vertex in the plane transverse to the beamline. Decay length significance is defined as $L_{xy}/\sigma_{L_{xy}}$, where $\sigma_{L_{xy}}$ is the uncertainty on L_{xy}.
[9] V. Abazov *et al.*, FERMILAB-PUB-05-034-E (2005).
[10] DØ Collaboration, V. Abazov *et al.*, hep-ex/0504043.
[11] We use the iterative, seed-based cone algorithm including midpoints, as described on p. 47 in G. C. Blazey *et al.* , in Proceedings of the Workshop: *"QCD and Weak Boson Physics in Run II",* edited by U. Baur, R. K. Ellis, and D. Zeppenfeld, FERMILAB-PUB-00-297 (2000).
[12] V. Barger, J. Ohnemus, and R.J.N. Phillips, Phys. Rev. D **48**, 3953 (1993).
[13] DØ Collaboration, B. Abbott *et al.*, Phys. Rev. D **58**, 052001 (1998).
[14] DØ Collaboration, S. Abachi *et al.*, FERMILAB-Conf-03/200-E.
[15] P. Sinervo, in *Proceedings of Statistical methods in Particle Physics, Astrophysics, and Cosmology*, edited by L. Lyons, R. P. Mount, and R. Reitmeyer (SLAC, Stanford, 2003), p. 334.